Development 127, 5285-5295 (2000)
Printed in Great Britain © The Company of Biologists Limited 2000
DEV2644

The WNT antagonist cSFRP2 modulates programmed cell death in the developing hindbrain

Debra L. Ellies[1,*], Vicki Church[2], Philippa Francis-West[2] and Andrew Lumsden[1]

[1]MRC Centre for Developmental Neurobiology, and [2]Department of Craniofacial Development, King's College London, Guy's Campus, London, SE1 1UL, UK

*Author for correspondence at present address: Stowers Institute for Medical Research, 1000E 50th Street, Kansas City, MO 64110, USA

Accepted 13 October; published on WWW 14 November 2000

SUMMARY

In the avian hindbrain, the loss of premigratory neural crest cells from rhombomeres 3 and 5 (r3, r5) through programmed cell death contributes to the patterning of emigrant crest cells into three discrete streams. Programmed cell death is induced by the upregulation of *Bmp4* and *Msx2* in r3 and r5. We show that cSFRP2, a WNT antagonist, is expressed in the even-numbered rhombomeres and that over-expression of *cSfrp2* inhibits *Bmp4* expression in r3 and r5, preventing programmed cell death. By contrast, depleting cSFRP2 function in r4 results in elevated levels of *Msx2* expression and ectopic programmed cell death, as does overexpression of *Wnt1*. We propose that programmed cell death in the rhombencephalic neural crest is modulated by pre-patterned *cSfrp2* expression and a WNT-BMP signalling loop.

Key words: Neural crest cell, Programmed cell death, Wnt, Chick

INTRODUCTION

Genetic studies in *C. elegans*, *Drosophila* and mouse have identified genes, such as *Ced3* (Yuan and Horvitz, 1990) and *Caspases* (Tewari et al., 1995), that are required for the conserved intracellular pathway leading to programmed cell death (PCD) (Jacobson et al., 1997). The mechanisms responsible for activating this death programme during development are tissue-specific, and although poorly understood, parts of the signalling mechanism have been identified for some tissues. Thus, Graham et al. (1994), Yokouchi et al. (1996), Zou and Niswander (1996), Ganan et al. (1996) and Merino et al. (1999) have demonstrated that BMP4 is sufficient to induce PCD in the rhombencephalon and interdigital mesenchyme. BMP4 induces PCD via a *Msx2*-mediated pathway during rhombencephalic and interdigital development, and in P19 cells (Graham et al., 1993; Zou and Niswander, 1996; Ganan et al., 1998; Marazzi et al., 1997). Yet, some studies on interdigital PCD have shown that *Msx2* regulates *Bmp4* expression (Ferrari et al., 1998). However, all data support the notion that BMP4 protein and *Msx2* overexpression lead to an increase in PCD, both in the rhombencephalon and interdigital mesenchyme (Takahashi et al., 1998; Ferrari et al., 1998; Buckland et al., 1998; Yokouchi et al., 1996; Marazzi et al., 1997; Merino et al., 1999), and their attenuation leads to neural tube defects, and abnormal digit patterning or webbing (Foerst-Potts and Sadler, 1997; Winograd et al., 1997; Katagiri et al., 1998; Ganan et al., 1998).

The developing hindbrain, which is metamerically subdivided into eight rhombomeres (r; Lumsden, 1990), produces premigratory neural crest (NC) cells along its dorsal margin, the majority of which migrate ventrally to the branchial arches. However, studies on the chick embryo have shown that the odd-numbered rhombomeres, r3 and r5, do not significantly contribute NC cells (Lumsden et al., 1991). Rather, r3 and r5 NC cells undergo PCD in both birds (Lumsden et al., 1991, Jeffs et al., 1992; Graham et al., 1993; Graham et al., 1994; Maden et al., 1997; Takahashi et al., 1998) and mouse (Serbedzija et al., 1996), sculpting discrete streams of r2, r4 and r6 NC cells from the otherwise continuous outflow from the dorsal neural tube. Those r3 and r5 NC cells that escape PCD may exit the neural tube either anteriorly or posteriorly at the adjacent rhombomere boundaries to join the NC streams from even-numbered rhombomeres (Sechrist et al., 1993; Birgbauer et al., 1995; Kulesa and Fraser, 1998). Those that contribute to the r4 NC stream may be incorporated in second branchial arch derivatives (Köntges and Lumsden, 1996). Those that migrate to join the r2 and r6 streams have been shown, by short-term labelling, to migrate 'towards' but not into branchial arch 1 nor 3 (Sechrist et al., 1993; Birgbauer et al., 1995; Nieto et al., 1995; Kulesa and Fraser, 2000). However, a study by Couly et al. (1996) based on grafting quail neural folds into chick hosts has shown that r3/r5 NC cells do make a small contribution to first and third branchial arches and later contribute to the intracartilaginous interfaces between r2 and r4 NC-derived cells (r3 derivatives) and between r4 and r6 NC-derived cells (r5 derivatives). However, another long-term r3 and r5 NC fate map has shown that r3 and r5 NC cells contribute only to the neuronal derivatives of r2 and r6 NC streams and not to first or third branchial arch structures

(Köntges and Lumsden, 1996). The discrepancies between Couly et al. (1996) and Köntges and Lumsden (1996) could be due to the stage of rhombomere transplantation, as cells within neighbouring rhombomeres have been shown to mix prior to rhombomere boundary formation (Fraser et al., 1990; Lumsden, 1990, 1991). Thus transplantation prior to rhombomere boundary formation, i.e. at 5 somites, leads to donor cells mixing with neighbouring host cells. Normally, the streamed NC cell emigration pattern, created at least in part by PCD, may play a role in keeping the distinct NC cell subpopulations from mixing with each other (Graham et al., 1996) as they enter and populate their respective first, second and third branchial arch territories.

The expression of *Msx2* and *Bmp4* has been shown to be tightly correlated with PCD in r3 and r5, both spatially and temporally (reviewed by Graham et al., 1996; Takahashi et al., 1998). When these odd-numbered rhombomeres are cultured in isolation, expression of *Bmp4* is downregulated and the PCD program is abrogated, thereby allowing the production of viable NC (Graham et al., 1993, 1994). When BMP4 protein is added to odd-numbered rhombomeres cultured in isolation, *Msx2* expression is upregulated and the PCD program restored (Graham et al., 1994; reviewed by Graham et al., 1996; Marazzi et al., 1997; Farlie et al., 1999). Yet, when r3 is co-cultured with an even-numbered rhombomere, *Bmp4* is expressed in r3 and NC cells undergo PCD (Graham et al., 1994), suggesting that *Bmp4* is regulated by an interaction with the even-numbered rhombomeres (reviewed by Graham et al., 1996). Yet, r3 is not freed from its PCD fate when it is isolated prior to rhombomere boundary formation, and even-numbered rhombomeres cannot induce PCD in odd-numbered rhombomeres, in vitro, if the rhombomeres are isolated independently and re-conjoined in vitro (Farlie et al., 1999). Thus, BMP4 (through *Msx2*) seems to play a significant role in initiating the PCD program, following an inductive signal from the even-numbered rhombomeres.

When even-numbered rhombomeres are treated with recombinant BMP4 protein, the PCD program is not initiated (Graham et al., 1994). By contrast, *Msx2* gain-of-function studies report that the NC of even-numbered rhombomeres can undergo PCD (Takahashi et al., 1998). Therefore, BMP4 is not capable of functioning alone and requires a co-factor to induce the *Msx2*-mediated PCD program within even-numbered rhombomeres.

Factors that could play a role in modulating PCD in the odd-numbered rhombomeres are members of the WNT family, as WNT signalling has been shown to inhibit *Bmp4* expression (Baker et al., 1999). The *Wnt* gene family consists of at least 16 members of secreted glycoproteins. They are thought to act through membrane bound frizzled receptors and have been shown to control cell fate and proliferation during embryogenesis (Parr and McMahon 1994; Hays et al., 1997; Saint-Jeannet et al., 1997; Yoshikawa et al., 1997; Moon et al., 1997; Dorsky et al., 1998). Recently, a group of putative WNT antagonists known as Secreted Frizzled Related Proteins (SFRPs) have been identified (Shirozu et al., 1996; Rattner et al., 1997; Melkonyan et al., 1997; Finch et al., 1997; Leynes et al., 1997; Salic et al., 1997; Xu et al., 1998; Chang et al., 1999). These proteins contain a cysteine rich domain, homologous to that found in the WNT frizzled receptors, and have been shown to bind WNTs (Lescher et al., 1998; Wang et al., 1997, 1997; Ladher et al., 2000). To date, six SFRP family members have been identified in human, mouse and chick. Several *Wnt* genes, including *Wnt1* and *Wnt3a* are expressed in the hindbrain (Hollyday et al., 1995), and *Sfrps* have been reported to be expressed in alternating stripes within the mouse rhombencephalon (Leimeister et al., 1998; Hoang et al., 1998). Furthermore, some of SFRP family members (SARP1, SARP2, and SFRP2) have been shown to indirectly modulate cellular responses to pro-apoptotic stimuli (Melkonyan et al., 1997; Wolf et al., 1997; Zhou et al., 1998*)*. These data raise the possibility that endogenous WNT antagonists may modulate PCD in the rhombencephalon. To investigate this, we have analysed the function of the chick SFRP2 homologue, cSFRP2. We show the temporal and spatial origins of the rhombencephalic PCD induction signal. In addition, we show that ectopic *cSfrp2* expression prevents PCD in the odd-numbered rhombomeres and its absence from the odd-numbered rhombomeres allows PCD to be induced. We therefore propose that rhombencephalic PCD is mediated by WNT signalling.

MATERIALS AND METHODS

Dorsal rhombomere ablations

Hi-Sex Brown eggs (J. K. Needle and Co, Waltham, Herts, UK) were incubated at 38±1°C with 50-60% (v/v) relative humidity to HH stages 8-10 (Hamburger and Hamilton, 1951), as PCD is first detectable with Acridine Orange at stage 9+ (unpublished observation). Using a flame-sharpened 100 μm tungsten wire, transverse cuts (3/4 of the rhombomere depth) were made along the rhombomere encompassing the even-numbered rhombomere to be excised. Embryos were then re-incubated to HH 11-13, whilst PCD is still detectable. The embryos were harvested and stained with Acridine Orange as previously described by Graham et al. (1993).

Nuclepore filter insertion

Hi-Sex Brown eggs were incubated at 38±1°C with 50-60% (v/v) relative humidity to HH stages 8-10. Using a flame-sharpened 100 μm tungsten wire, one transverse cut was made along a rhombomere boundary. A 0.015 μm pore size, or a non-porous Nuclepore filter (Costar), was placed into the cut and embryos were then re-incubated until HH 11-13. The embryos were then harvested and stained with Acridine Orange as previously described by Graham et al. (1993).

Construction of the *cSfrp2* retrovirus

The *cSfrp2* coding region was amplified from the chick *cSfrp2* cDNA (Ladher et al., 2000) by PCR, using oligonucleotide primers to the 5′ ORF sequence CCGCCATG**G**CGCGCCGCCTC and 3′ ORF sequence CCAAAGCTTCTAACACTGCAGT. The PCR program consisted of 35 cycles of three steps: 95°C for 1 minute, 60°C for 1 minute, and 72°C for 1 minute. The *Nco*I/*Hin*dIII *cSfrp2* fragment was then subcloned into the adaptor plasmid pSlax12Nco RCAS subtype B containing *cSfrp2* was then created using *Cla*I/pSLAX12Nco and its orientation was determined by restriction digest analysis and nucleotide sequencing.

Explanted rhombomeres

Hi-Sex Brown eggs were incubated at 38±1°C with 50-60% (v/v) relative humidity to HH 10. The odd-numbered rhombomeres were injected by mouth with DiI and the rhombomeres were isolated as described by Graham et al. (1993). The isolated rhombomeres were then cultured with either cSFRP2- or green fluorescent protein (GFP)-conditioned medium from chick embryo fibroblasts (CEF) infected with either RCAS(B)-EGFP (kindly provided by J. Gilthorpe) or

RCAS(B)-*cSfrp2*. GFP was used as a control to also determine whether supernatant containing the retrovirus could infect the explanted rhombomeres. The CEFs were $CaCl_2$-transfected and grown as described by Morgan and Fekete (1996).

HNK-1 immunochemistry

The explants were fixed and processed as described by Graham et al. (1993), with the following modifications. The entire procedure was performed without detergent as HNK-1 is a cell surface molecule. The HNK-1 antibody (Zymed 07-5703) was added at a dilution of 1:200 and incubated overnight at 4°C. The secondary antibody was a goat anti-mouse FITC (Jackson IRL, 115-096-044) diluted at 1:200 and was incubated for 1 hour at room temperature. The explants were viewed using confocal microscopy.

Whole-mount in situ hybridization

A minimum of five embryos per stage were assayed for all whole-mount in situ hybridization experiments. The in situ protocols used were as described by Grove et al. (1998) with the following modifications. The synthesis of the RNA was extended from 2 hours to 4 hours, and the hybridization step was carried out for 48 hours instead of 18 hours. Explants were processed as whole mounts, however, they were first covered with an 8% gelatin solution, and hybridised for 12 hours only.

cDNA for making riboprobes

An 800 bp mouse *Krox20* partial cDNA, containing the zinc finger and 3′UTR, was used as a template (Wilkinson 1992) for antisense transcription. A 700 bp *Eco*RI-*Hin*dIII chick *Hoxb*2 partial 3′cDNA fragment was used as a template for antisense transcription (kindly provided by A. Kuroiwa, Japan). A 600 bp mouse *Fgf8* partial cDNA fragment was used as a template for antisense transcription (Mahmood et al., 1995). A 5′ 350 bp chick *Msx2* partial cDNA fragment was used as a template for antisense transcription (Graham et al., 1993). A 1 kb chick *Bmp4* partial cDNA fragment was used as a template for antisense transcription (Francis et al., 1994). A 1.68 kb chick *cSfrp2* cDNA fragment was used as a template for antisense transcription. A 500 bp chick TCF4 partial cDNA encoding a fragment between the conserved HMG box and β-catenin binding domain was used as a template for antisense transcription (kindly provided by L. Paganess and C. Tabin, Harvard University, USA). The *Wnt1* cDNA was used for antisense transcription as described by Hollyday et al. (1995).

The *cSfrp2* whole-mount in situ hybridized embryos were vibratome sectioned at 60 μm according to standard procedures.

Electroporation

Electroporation of retroviral constructs was used instead of viral infection methods because we required expression of the constructs by HH 9-10, and traditional infection methods would have yielded low infection and high mortality rates. The RCAS(B)-EGFP construct (kindly provided by J. Gilthorpe) was either electroporated alone or co-electroporated with either RCAS(B)-*Wnt3a* (kindly provided by C. Tabin; Kengaku et al., 1998) or RCAS(A)-*Wnt1* (kindly provided by A. Brown (Rudnicki and Brown, 1997) or RCAS(B)-antisense *cSfrp2*. A dual pulse isolated stimulator (Intercept TSS10) and silver electrodes were used to electroporate (20 volts) the constructs into HH 6-7 chick hindbrains in ovo. Each electroporation contained a solution of 0.5 μg/μl of each DNA construct and 0.06% Fast Green dye dissolved in 1×PBS.

RESULTS

Cell death is induced in an anterior-to-posterior wave

In vitro studies have shown that BMP4/*Msx2* are implicated in the PCD of odd-numbered rhombomere NC cells that is induced by the even-numbered rhombomeres (Graham et al., 1993, 1994). To further examine this phenomenon, we performed in vivo ablations of the dorsal part of even-numbered rhombomeres to determine the precise timing of PCD induction from the even-numbered rhombomeres.

Even-numbered rhombomeres were ablated at HH 8-10 (Fig. 1A,B) and the embryos were allowed to develop until HH 11-13. They were analysed for cell death by Acridine Orange (AO) staining and simultaneously for the expression of gene markers by whole-mount in situ hybridization. Following dorsal ablations, the expression of either *Hoxb2*/*Krox20* or *Fgf8*/*Krox20* was determined to ensure that the correct even-numbered rhombomere had been removed. In all cases, *Hoxb2*/*Krox20* and *Fgf8*/*Krox20* expression was as anticipated

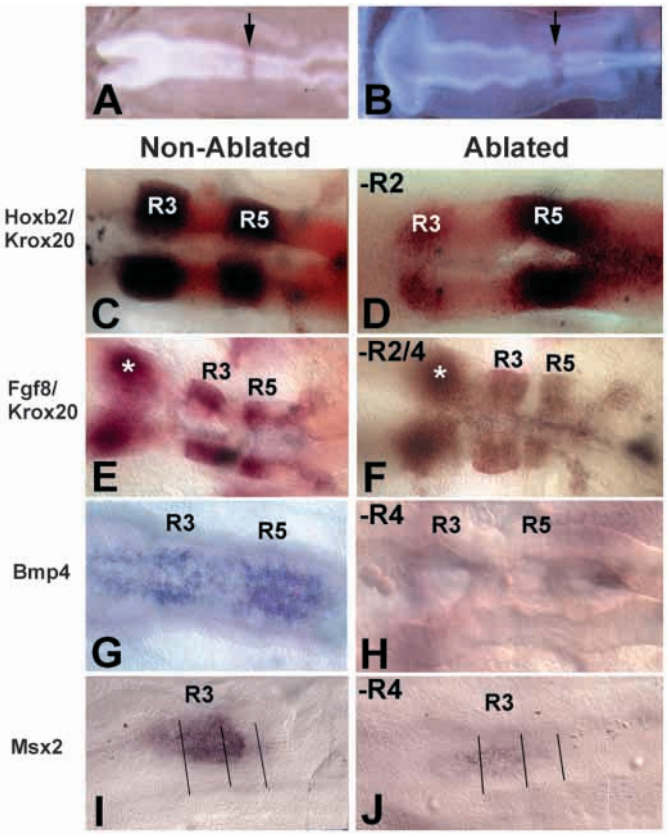

Fig. 1. Even-numbered rhombomere ablations lead to down-regulation of *Bmp4* and *Msx2* expression. All panels shoe dorsal views with anterior to the left. (A,B) Chick hindbrains at (A) HH 8 with r2 ablated (arrow), or (B) HH 10 with r4 ablated (arrow). (C,E,G,I) Control non-ablated embryos showing expression of (C) *Krox20* (blue) and *Hoxb*2 (red) in a HH 11 embryo; (E) *Krox20* (blue) and *Fgf*8 (asterisk, red) in a HH 12 embryo; (G) *Bmp4* (blue) and (I) *Msx2* (blue) in a HH 11 embryo. (D,F,H,J) Experimental embryos with ablated rhombomeres. (D) HH 11 embryo from which r2 had been ablated at HH 8, showing a loss of *Krox20* expression in r3. (F) HH 12 embryo that had both r2 and r4 ablated at HH 10 showing unchanged expression of *Fgf*8 (asterisk) and *Krox20* genes. (H) HH 11 embryo from which r4 had been ablated at HH stage 10, showing a loss of *Bmp4* expression. (J) HH 11 embryo from which r4 had been ablated at HH 10, showing a down-regulation of *Msx2* expression. R3 and R5, rhombomeres 3 and 5 in this and subsequent figures; black lines in (I,J) demarcate rhombomere boundaries.

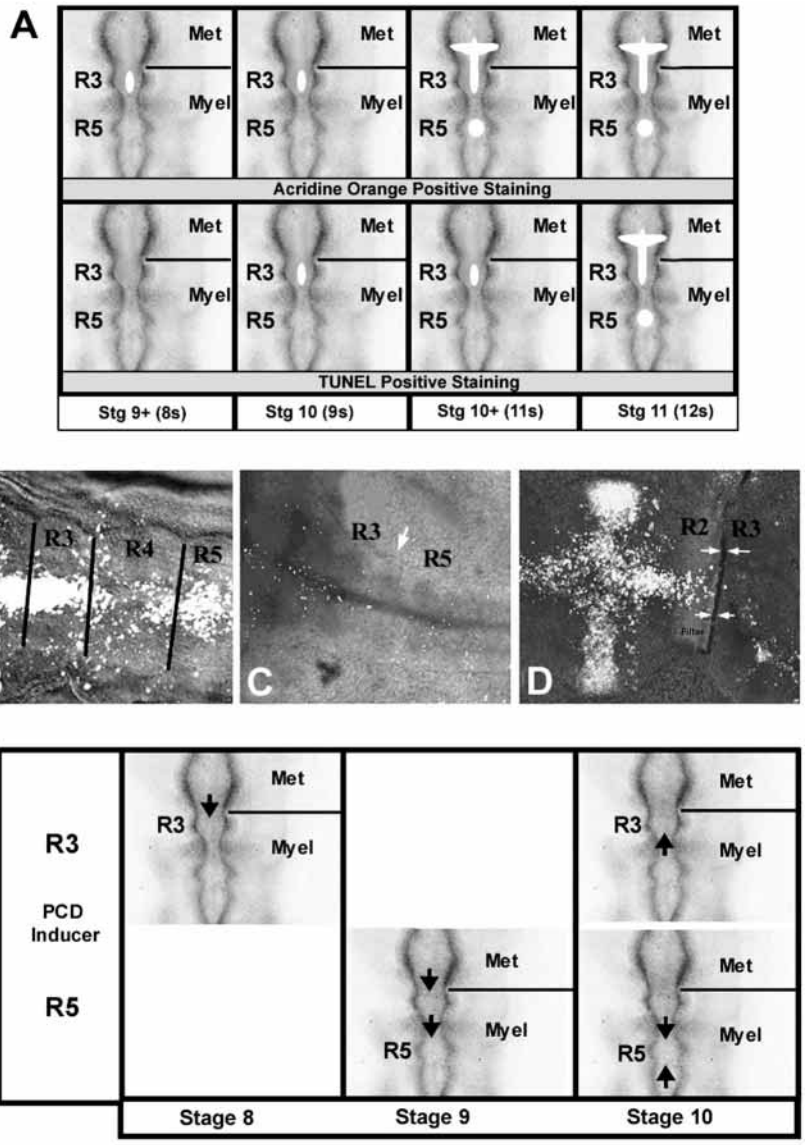

Fig. 2. Rhombencephalic cell death occurs in an anteroposterior wave. (A) Spatial and temporal comparison of r3 and r5 cell death using Acridine Orange and TUNEL staining (semi-diagrammatic). (B-D) Dorsal views of chick hindbrains with anterior to the left. Acridine Orange-positive cells appear white. (B) Control embryo at HH 11; rhombomere boundaries marked by lines. (C) A HH 11 embryo from which r4 had been ablated at HH 10 (arrowed) showing a loss of Acridine Orange-positive cells in r3 and r5. (D) HH 11 embryo that had a non-porous filter inserted between r2 and r3 at HH 8, showing a decrease in the levels of cell death in r3. Arrows point to the width of the filter which has tilted out of perpendicular during flat mounting, such that the deeper part of the filter has become inclined anteriorly and thus visible in the micrograph. (E) Summary of the ablation data. The r3 death-inducing signal starts at stage 8 from r2 (arrow), and than at stage 10 from r4, whereas, the r5 death-inducing signal starts at stage 9 from both r2 and r4, then at stage 10 from r4 and r6. Met, metencephalon; Myel, myelencephalon.

(compare Fig. 1E,F), except that *Krox20* is down-regulated in r3 after r2 ablation at HH 8. *Hoxb2* expression, however, was normal (compare Fig. 1C,D), indicating that the down regulation of *Krox20* expression in r3 was not due to its removal. A gap between the *Krox20* expression in r3 and r5 is seen in the basal plate of r4 that was not removed.

An analysis of TUNEL and AO staining has revealed that they both identify the same spatial pattern of PCD in the avian hindbrain (data not shown). However, AO stains slightly younger staged embryos (Fig. 2A). This is not surprising because AO is specific for condensing chromatin, a characteristic that appears earlier than the 3′ DNA nicks detected by TUNEL. In addition, it appears that TUNEL is not specific for cells undergoing PCD, as cells undergoing necrosis also stained positive for TUNEL (Grasl-Kraupp et al., 1995). The spatial pattern of PCD seen with AO in the avian hindbrain starts in r3 at the 8-somite stage, and at the 10-somite stage AO+ cells are found in r2 and at the boundary between r1/r2 (Fig. 2A). This anterior pattern of cell death then persists until HH stage 13 and the posterior pattern of cell death, specifically in r5, begins at 11 somites according to AO staining (Fig. 2A). By HH stage 12, the anterior and posterior patterns are both present and additional AO+ cells can be seen in the r4 and r6 NC migratory routes. AO+ cells are not found after HH stage 13 in the rhombencephalon. In vitro analysis and homotopic grafting has revealed that AO+ cells in adjoining even-numbered rhombomeres originate from the odd-numbered rhombomeres (unpublished observation; Graham et al., 1993).

Ablation of r2 at HH 8 resulted in a 50% reduction in r3 PCD, while it had no effect on r5 (Table 1). Removal of the other even-numbered rhombomeres (r4 or r6) did not effect PCD in either r3 or r5.

By contrast, ablation of any even-numbered rhombomere at HH 9 had no effect on the levels of PCD in r3. However, removal of r2 at the 6-somite stage (HH 9–) or r4 at the 8-somite stage (HH 9+) resulted in a 70% reduction in the level of PCD in r5 (Table 1). Ablation of r6 had no significant effect on either r3 or r5 PCD.

The most robust effect on the levels of PCD in either r3 or r5 was seen after ablating r4 at HH 10. After r4 ablation, r3 PCD was reduced by 78% (Fig. 2C; Table 1), and r5 PCD was reduced by 90% (Fig. 2C; Table 1). At this stage the level of PCD within r3 or r5 was not affected by removal of r2. While loss of r6 had no effect on r3 PCD, PCD in r5 was reduced by 76% (Table 1).

Msx2 and *Bmp4* expression was analysed to verify that this reduction of PCD in r3 and r5 is accompanied by a decrease in PCD-mediating molecules (Graham et al., 1993, 1994). In all embryos in which r4 had been ablated at HH 10, *Bmp4* (n=17) and *Msx2* (n=29) expression was lost in r3 and r5 (Fig. 1G-J), as expected (Graham et al., 1993, 1994).

Therefore, the first detectable induction of PCD in r3 arises

Table 1. Mann-Whitney 2-tailed statistical significance (*P* value) of PCD, in r3 and r5, after even-numbered rhombomere ablation

	r3		r5	
Ablation	*P*-value	% PCD reduction	*P*-value	% PCD reduction
HH Stage 8				
r2 (*n*=10)	0.026	50	0.12	0
r4 (*n*=5)	0.18	0	0.18	0
r6 (*n*=8)	0.12	0	0.12	0
HH Stage 9				
r2 (*n*=12)	0.3	0	0.06	72
r4 (*n*=11)	0.15	0	0.06	67
r6 (*n*=5)	0.14	0	0.3	0
HH Stage 10				
r2 (*n*=11)	0.3	0	0.7	0
r4 (*n*=10)	0.04	78	0.018	90
r6 (*n*=10)	0.5	0	0.06	76

at HH 8 from r2 and switches to r4 at HH 10 (Fig. 2E). In the case of r5, the first detectable induction of PCD arises at HH 9 from r2 at the 6-somite stage and from r4 at HH 9+ (Fig. 2E). Subsequently, this signal shifts to r4 and r6 at HH 10 (Fig. 2E). Thus, the PCD inducing signals seem to follow an anteroposterior wave of maturation similar to that of neural crest emigration.

Neural crest cell death is mediated by a diffusible molecule

To further characterise the PCD signal arising from the even-numbered rhombomeres, barriers were inserted at rhombomere boundaries. Either non-porous or porous (0.015 μm pore diameter) Nuclepore filters were used to test the effect of blocking signal transmission and to distinguish between diffusible and cell contact-mediated signals.

Filters were inserted when the even-numbered rhombomeres begin to transmit their PCD inducing signals. Insertion of non-porous filters in the r2/3 boundary (*n*=11) at HH 8, in r4/5 (*n*=19) at HH 9-10, and in r3/4 (*n*=13) at HH 10, resulted in an 80% reduction of PCD within either r3 or r5 (*n*=31/35; Fig. 2D). This confirmed results from the ablation of even-numbered rhombomeres. By contrast, the insertion of porous filters at equivalent positions and stages did not change the level of PCD in either r3 or r5 (*n*=27/32; data not shown). Therefore, the even-numbered rhombomeres produce a diffusible signal between HH 8-10 (Fig. 2E), which induces PCD in the NC of r3 and r5. Although the even-numbered rhombomeres produce an apoptotic-inducing signal, they do not undergo PCD themselves. Secreted proteins that are candidates for the role of apoptotic inducers include members of the SARP family (Melkonyan et al., 1997), which includes several secreted frizzled-related proteins (SFRPs) (Leimeister et al., 1998). We therefore analysed the expression of chick *Sfrp* homologues in the hindbrain.

PCD is controlled by a WNT-BMP loop

cSfrp2 is initially expressed throughout the hindbrain (HH 7-9–; Fig. 3A,B) but is subsequently down-regulated in the odd-numbered rhombomeres at HH 9 (Fig. 3C,D). Expression in the even-numbered rhombomeres at HH 9+-12 is graded, being highest at the ventricular side and lowest at the pial side of the dorsolateral neural tube (Fig. 3D). The timing of this down-regulation correlates closely with the onset of PCD in the odd-numbered rhombomeres, thus suggesting that cSFRP2 may diffuse to the dorsal neural tube.

To investigate whether the down-regulation of *cSfrp2* in the odd-numbered rhombomeres is sufficient to induce PCD, we cultured DiI-labelled HH 10 r3 explants in medium conditioned either by cells expressing cSFRP2 from a retrovirus or by control cells expressing GFP from a retrovirus. r3 explants cultured in medium conditioned by control cells produced many DiI-labelled NC cells (53% of total NC cells were labelled with DiI; *n*=5; Fig. 4E). The addition of medium conditioned by cSFRP2-expressing cells altered neither the total number of migratory NC cells nor DiI-labelled r3 neural crest cells (*n*=6; Fig. 4E). Thus, exogenous cSFRP2 does not affect the number of r3 neural crest cells produced when r3 is rescued from PCD.

However, a dramatic effect was seen with exogenous cSFRP2 when DiI-labelled r3 explants were cultured in conjunction with r4, which normally induces cell death in r3 (Graham et al., 1994). cSFRP2-conditioned medium prevented PCD of r3 NC when co-cultured together with r4 (40% of the total neural crest was labelled with DiI, *n*=5; Fig. 4C,E) whereas control conditioned medium did not alter r3 neural crest PCD (4% of the total neural crest was labelled with DiI, *n*=6; Fig. 4A,E). Thus, cSFRP2 seems to function by inhibiting the effect of the PCD inducer arising from the even-numbered rhombomere.

To verify that cSFRP2 was acting by inhibiting PCD in the explants, we analysed the expression of *Bmp4*. In the control cultures, *Bmp4* expression was found in 83% of explants (*n*=5/6, Fig. 4B), whereas in the explants cultured in cSFRP2-conditioned medium, *Bmp4* expression was extinguished in 63% of explants (*n*=5/8, Fig. 4D). Thus, cSFRP2 causes a loss of *Bmp4* expression, which is known to be sufficient to induce rhombencephalic cell death (Graham et al., 1994).

To ascertain whether cSFRP2 is required to prevent PCD in the even-numbered rhombomeres, we sought to knockdown cSFRP2 by electroporation of retroviral antisense *cSfrp2*. Each set of constructs was electroporated in conjunction with a GFP-expressing retrovirus, to monitor electroporation efficiency. The electroporated embryos were then assayed for PCD and subsequently for expression of genes known to be involved in rhombencephalic PCD, and controlled using the level of *Sfrp2* mRNA. In control HH 6-7 GFP electroporated embryos, the levels of PCD and *Msx2* expression were unchanged from that seen in uninjected embryos (*n*=10/14; Fig. 5A,B), and GFP

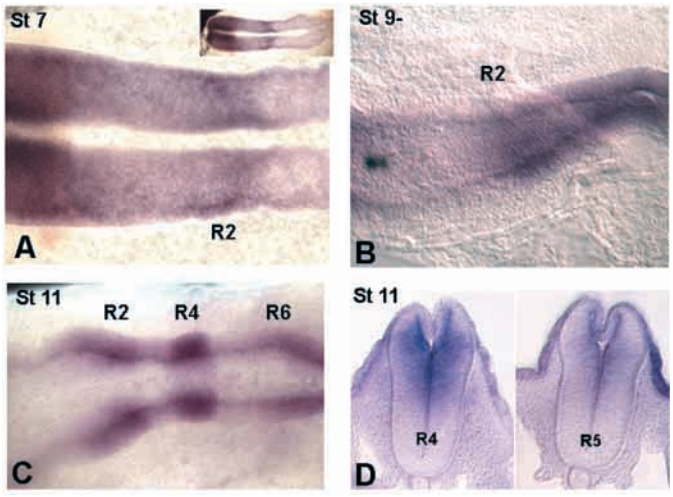

Fig. 3. *cSfrp2* expression patterns in the developing rhombencephalon. Dorsal views of a chick rhombencephalon with anterior to the left. (A) HH 7 embryo showing *cSfrp2* expression (blue-brown) in the cranial neural folds. Rhombomere 2 (R2) is indicated. (B) HH 9– embryo showing *cSfrp2* expression throughout the hindbrain. (C) HH 11 embryo showing *cSfrp2* expression is downregulated in the odd-numbered rhombomeres. (D) Coronal sections (dorsal to the top) through either r4 or r5 showing *cSfrp2* expression is strongest in the ventricular layer of r4, whereas *cSfrp2* is downregulated in r5.

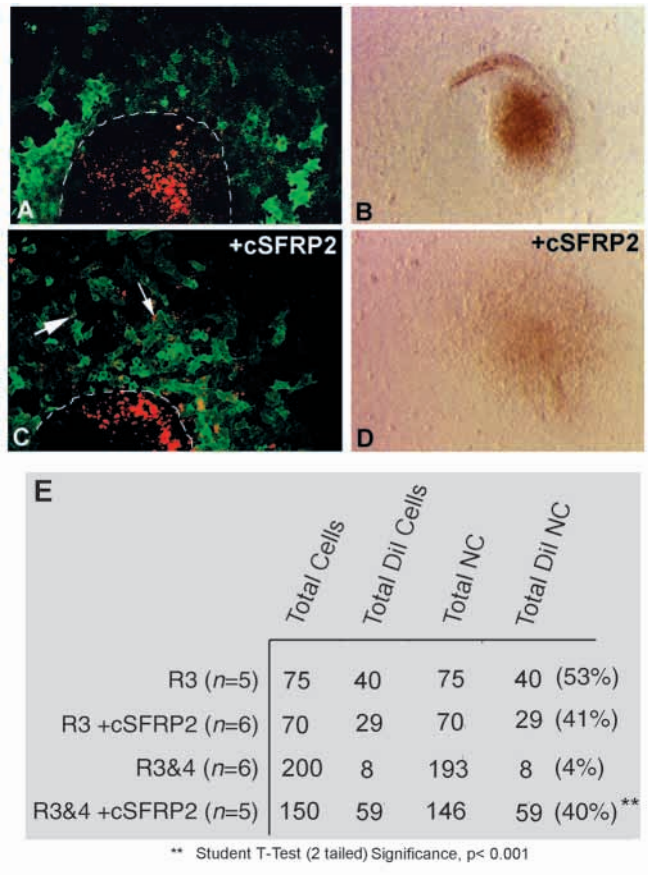

Fig. 4. cSFRP2 inhibits NC death and downregulates *Bmp4* expression. HH 10 DiI-labelled (red) r3 cultured in conjunction with r4, and then stained for HNK-1 (green). The location of the explant is marked with a dashed white line in A and C. (A,B) r3 and r4 cultured in the presence of GFP-conditioned medium or (C,D) cSFRP2-conditioned medium. Compare the number of DiI-labelled r3 and HNK-1 cells migrating out of the explants in A and C. Arrows point to double-labelled NC cells that are DiI and HNK-1 positive. (B,D) The explants were assayed for *Bmp4* expression (brown). In the control cultures, *Bmp4* is expressed (B) whereas in cSFRP2 conditioned cultures *Bmp4* is downregulated (D). (E) Summary of the rhombomere explant data. The total number of cells was detected using phase microscopy; Total DiI Cells are DiI cells from r3 that are migratory; Total NC Cells are the HNK-1-positive cells; Total DiI NC are the cells that are positive for both DiI and HNK-1. *Student's *t*-test (2-tailed) significance of $P<0.001$.

was found in bilateral patches of the hindbrain (insert, Fig. 5A). Therefore, the electroporation procedure did not lead to any changes in the levels of PCD within the rhombencephalon.

HH 6-7 embryos were used for electroporation of antisense *cSfrp2*. We found that the majority of embryos were normal in appearance and the hindbrains that showed high levels of GFP were assayed for PCD using Acridine Orange, *Sfrp2* and *Msx2* expression. An increase in PCD was seen in 96% of embryos ($P<0.005$, $n=21/22$) and elevated *Msx2* expression ($n=17/17$) within r4 at HH 11 (Fig. 5E,F), and in the lateral neural tube. The level of *Sfrp2* mRNA was drastically reduced in embryos that were injected with antisense *Sfrp2* (Fig. 5F), thus the antisense *Sfrp2* was binding sufficiently to the sense *Sfrp2* mRNA and causing its degradation by RNase-H. Intriguingly, we observed a marked increase in the levels of PCD and *Msx2* expression in the dorsolateral neural tube, where *cSfrp2* is normally expressed (Fig. 5E,F), indicating that the antisense *cSfrp2* was also functioning at the exact site of *cSfrp2* expression.

cSFRP2 is known to act as an antagonist of WNT8 (Ladher et al., 2000). Therefore, another approach that should result in a loss of cSFRP2 function would be to overexpress a *Wnt* gene that is normally found in the hindbrain at the relevant stages; candidates include *Wnt3a* and *Wnt1*. When *Wnt3a* was electroporated into the hindbrain at HH 6-7 ($n=43$), embryos developed with abnormally flattened heads in 54% of cases ($n=23/43$). Of the remaining embryos ($n=20$), 4 developed with an open neural tube. In the embryos with high levels of co-electroporated GFP expression, levels of PCD were analysed, and 75% ($P<0.005$) of these had elevated levels of PCD ($n=15/20$) and *Msx2* expression ($n=8/10$) in r4 at HH 9-13. These effects were much more marked when *Wnt1* was electroporated, where all of the 9/11 embryos with strong GFP and *Wnt1* expression failed to close their neural tubes, and both *Msx2* expression and PCD were strongly upregulated in the open neural folds at all levels of the hindbrain, including r4 (Fig. 5C,D). Consistent with this, *cSfrp2* mRNA injected into *Xenopus* embryos antagonises the dorsalizing effects of WNT1 but not those of WNT3a (L. Dale and D. E., unpublished data).

Thus, both methods of interfering with cSFRP2 function, antisense knockdown and increasing the levels of ligand, resulted in increased PCD and elevated *Msx2* expression. In addition, cSFRP2 did not alter the total number of rhombomeric NC cells produced (see Fig. 4E).

Following reports that WNTs can signal either through a β-catenin-dependent or -independent pathway (Boutros et al., 1998; Li et al., 1999), and that the downstream WNT effector

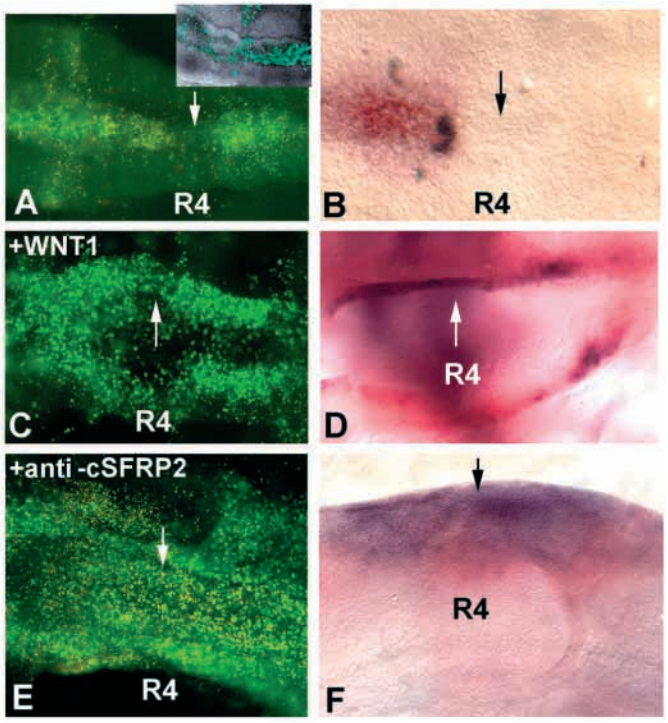

Fig. 5. cSFRP2 loss of function results in increased levels of PCD and *Msx2* expression within the rhombencephalon. Dorsal views of electroporated chick hindbrains with anterior to the left. (A,C,E) PCD as detected using Acridine Orange. (A) HH 10 embryo (similar at HH 11) shows PCD after a GFP control was electroporated (arrow points to apoptotic gap in r4), the top insert shows the GFP protein distribution after the electroporation. (C) HH 10 embryo showing increased levels of PCD in r4 (arrow) and along the neural folds, after *Wnt1* electroporation. (E) HH 11 embryo showing increased levels of PCD in r4 (arrow) and the lateral part of the rhombencephalon after electroporating antisense *cSfrp2*. (B,D,F) Expression of *Msx2* (blue) after electroporation of the above constructs. (B) *Msx2* expression is detected in r3 and r2 but not in r4 (arrow) at HH 10 after electroporation of a GFP control construct. (D) *Msx2* expression is upregulated in r4 (arrow) and adjacent neural folds after overexpression of *Wnt1*(red). (F) Lateral view of the chick rhombencephalon after antisense *cSfrp2* electroporation. *Msx2* expression is greatly increased in r4 (arrow) and *cSfrp2* expression (red) is diminished at HH 11 (compare with Fig. 3C). Electroporation of either *cSfrp2* antisense or *Wnt1* sense resulted in a Chi-squared significance of $P<0.005$.

Tcf4 is expressed in r3 and r5 in mouse embryos (Cho and Dressler, 1998), we set out to examine the possible role of TCF4 in NC PCD in chick. We first analysed the expression of *Tcf4* in normal embryos and then after altering the pattern of PCD. We found that, unlike in the mouse, *Tcf4* is expressed all along the cranial neural folds at HH 9 (6-somite stage), and throughout the HH 10+ hindbrain (data not shown). Following gain or reduction of cSFRP2 function, *Tcf4* expression was *Tcf4* is downregulated in the even-numbered rhombomeres (N=9/17), suggesting that *Tcf4* is transcriptionally repressed by WNT3a (data not shown). Thus, our preliminary results suggest that SFRP2 acts via a β-catenin-independent pathway.

DISCUSSION

The neural crest primordia of rhombomeres 3 and 5 undergo extensive PCD. The induction of PCD depends on the presence of even-numbered rhombomeres (Graham et al., 1993), and is influenced by BMP4 and *Msx2* (Graham et al., 1993, 1994).

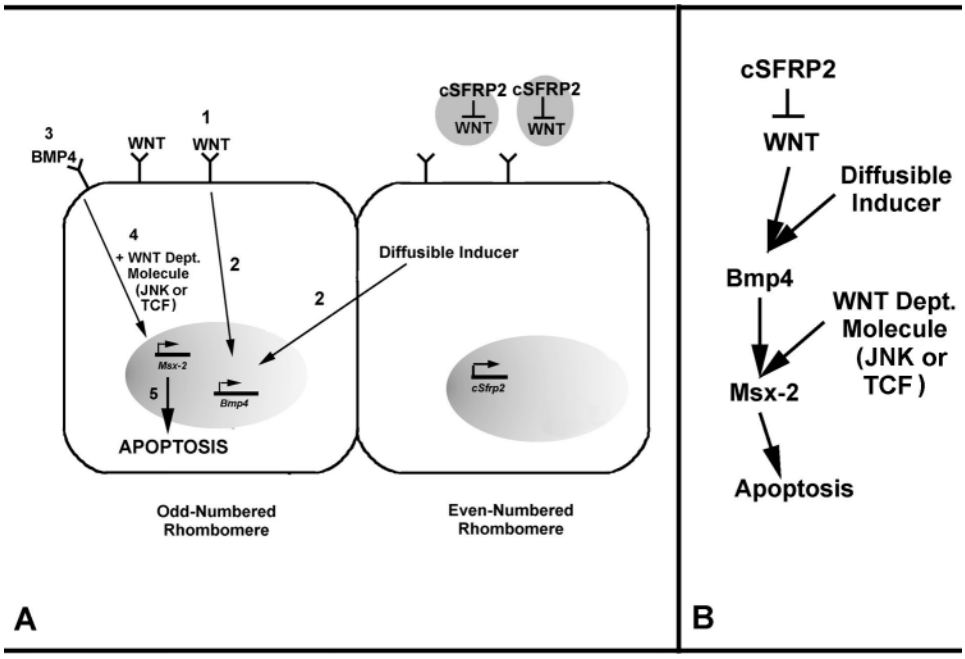

Fig. 6. Proposed model for rhombencephalic PCD. (A) Schematic representation of an even and odd-numbered rhombomere. The even-numbered rhombomere contains cSFRP2 protein, which antagonises the WNT's signalling. However, the even-numbered rhombomere produces a diffusible factor that acts (in the odd-numbered rhombomere) in combination with the WNT signalling (1) to activate *Bmp4* expression (2). BMP4 protein then acts on the odd-numbered rhombomere (3), and in conjunction with a WNT-dependent molecule (like TCF4 or JNK) activates *Msx2* expression (4). This in turn activates the PCD fate (5). (B) A simple view of the molecules involved. cSFRP2 antagonises WNT signalling, WNT signalling in conjunction with the even-numbered rhombomere's PCD-inducing signal activates *Bmp4* expression. BMP4 in conjunction with a WNT-dependent molecule activates *Msx2* expression and this leads to PCD.

However, the signalling cascade leading to PCD in the hindbrain is largely unknown. This study sheds further light on the induction of PCD, in particular the role of WNT signalling via the antagonistic effects of cSFRP2.

We have found that the even-numbered rhombomeres produce a secreted molecule that diffuses into the odd-numbered rhombomeres to induce PCD. We have identified r2 as the source of the early PCD-inducing signal for r3 at HH 8. Likewise, r4 is required to induce PCD in r5 at HH 9. In both cases, signalling occurs prior to the detection of PCD within the particular rhombomere, indicating that this early inducing signal is not the PCD execution signal. Rather, it is probably the initial signal necessary for the later execution signal at HH 10. The production of these early and late PCD signals by the even-numbered rhombomeres follows an anterior-posterior wave similar to that of subsequent neural crest emigration.

The secreted PCD-inducing molecule, while produced by the even-numbered rhombomeres, can apparently induce PCD only in rhombomeres 3 and 5. The even-numbered rhombomeres must therefore either contain an inhibitor against the induction of PCD, or they lack a co-factor required for the PCD inducer function. We propose that PCD in the even-numbered rhombomeres is actively inhibited, and that cSFRP2 is the molecule responsible for the inhibition. cSFRP2 has appropriate characteristics as a candidate effector of inhibition: it is expressed specifically in the even-numbered rhombomeres at the critical stages, and gain or reduction of function experiments indicate that cSFRP2 interferes with the PCD program. Gain of cSFRP2 function leads to loss of *Bmp4* expression and arrest of PCD in r3 and r5, whereas interference with cSFRP2 function leads to increase of *Msx2* expression in the even-numbered rhombomeres and the induction of PCD.

It is likely that cSFRP2 functions in the control of PCD via the suppression of WNT signalling (Shirozu et al., 1996; Rattner et al., 1997; Melkonyan et al., 1997; Finch et al., 1997; Leynes et al., 1997; Salic et al., 1997; Xu et al., 1998; Chang et al., 1999; Ladher et al., 2000; Lee et al., 2000). Involvement of SFRPs in PCD has been shown for mammary gland, ovarian corpus luteum and prostate (Wolf et al., 1997), breast adenocarcinoma (Melkonyan et al., 1997), and immortalized breast epithelial cells (Zhou et al., 1998).

Several *Wnt* genes are expressed in the developing hindbrain and are candidates for mediating PCD: *Wnt1* and *Wnt3a* are expressed along the dorsal midline of the hindbrain (Hollyday et al., 1995), whereas *Wnt8c* is restricted to the dorsal midline of r4 (Hume and Dodd 1993). Together, *Wnt1* and *Wnt3a* have been shown by overexpression or null mutation to function during NC induction; their involvement with NC PCD is therefore difficult to assess (Augustine et al., 1993; Ikeya et al., 1997; Saint-Jeannet et al., 1997; LaBonne and Bronner-Fraser, 1998). An analysis of PCD in the *Wnt1* and *Wnt1;Wnt3a* null mutants reported no change in hindbrain PCD (Serbedzija et al., 1996; Ikeya et al., 1997). However, contrary to the previous report of PCD in mouse r3 and r5 NC (Serbedzija et al., 1996), a recent examination has failed to detect this PCD (Trainor and Krumlauf, personal communication).

To determine whether or not *Wnt3a* and/or *Wnt1* function to modulate PCD in the chick rhombencephalon, we have analysed the effect of their overexpression. The embryos showed upregulation of PCD in the even-numbered rhombomeres, similar to the antisense reduction of cSFRP2 function. During normal hindbrain development, *Wnt1* and *Wnt3a* expression starts at HH 7, a stage when *cSfrp2* expression is ubiquitous. PCD would thus be prevented by cSFRP2 until, at HH 9, *cSfrp2* expression is downregulated in r3 and r5. At this stage and rhombomere level, WNT signalling is no longer antagonised and PCD is initiated.

We have found that WNT1 is more effective than WNT3a at increasing levels of *Msx2* expression and PCD in the neural folds. This is consistent with the findings of Lee et al. (2000), who showed that mSFRP2-expressing cells antagonise the dermomyotome-inducing activity of WNT1 and WNT4, but not that of WNT3a. Furthermore, cSFRP2 antagonises the dorsalizing activity of WNT1 but not that of WNT3a in *Xenopus* assays (L. Dale and D. E., unpublished data).

Previous studies on the function of *Wnt* genes have not provided evidence for the involvement of a specific *Wnt* in hindbrain PCD, whereas their involvement has been shown in determining NC cell fate (Dorsky et al., 1998), expansion of NC populations (Saint-Jeannet et al., 1997; Ikeya et al., 1997), and neural tube closure (Augustine et al., 1993). These various effects on development could be attributed to the specific dose dependence effects of the WNT proteins (Dorsky et al., 1998; Wilder and Perrimon, 1995). Here, we have shown that both WNT3a and WNT1 could be involved in regulating PCD in r3 and r5. This is consistent with the phenotypes of *Wnt* mutant mice, which exhibit similar developmental defects to those seen when PCD is arrested, as in *Apaf1* mutant mice or caspase inhibition, which develop with incomplete fusion of the neural folds (Augustine et al., 1993; Yoshida et al., 1998; Weil et al., 1997). The effects may often be concealed, since *Wnt* genes act not only during neurulation and neural crest induction, but also during gastrulation; thus, *Wnt* mutant mice exhibit severe defects which are associated with this earlier event. *Wnt1* mutants show a loss of midbrain and cerebellar structures only (McMahon and Bradley, 1990).

WNT signalling activates dishevelled (DSH), which can then act along two distinct pathways: one of these involves antagonising ZestWhite-3 kinase/GSK3β to stabilise β-catenin and enable its nuclear translocation (reviewed by Shulman et al., 1998; Wodarz and Nusse 1998); the other pathway, independent of β-catenin, involves the kinases JNK/SAPK (Boutros et al., 1998; Li et al., 1999). JNK signalling is involved in inducing cell death in many cell types (reviewed by Basu and Kolesnick 1998). Furthermore, *Jnk* is expressed in the hindbrain of mice, and double *Jnk1;Jnk2* mutant mice have reduced PCD in the hindbrain and their neural folds fail to close (Kuan et al., 1999).

Further evidence for β-catenin-independent WNT signalling in hindbrain NC PCD comes from analysing other components of the β-catenin pathway, such as TCF4, which is required to bind β-catenin for nuclear translocation and transcription of target genes (Brannon et al., 1997; Brunner et al., 1997; reviewed by Eastman and Grosschedl 1999; Korinek et al., 1998). Our results indicate that *Tcf4* is expressed throughout the hindbrain at equivalent stages in chick, suggesting that during PCD, WNTs may signal through a β-catenin-independent pathway.

Our study indicates an important role for WNT signalling in the induction of PCD in the developing rhombencephalon. We have shown that *Bmp4* and *Msx2*, both closely associated with PCD, are downstream of WNT signalling. However, WNT

signalling alone appears not to be sufficient to cause PCD, since odd-numbered, *Wnt*-expressing rhombomeres cultured in isolation do not undergo PCD (Graham et al., 1993). Culturing r3 in conjunction with r4 in cSFRP2-conditioned medium, culturing r3 in isolation (Graham et al., 1994), or removing the PCD inducer originating from the even-numbered rhombomeres, all result in the down-regulation of *Bmp4* expression and arrest of r3 PCD. This indicates that the induction of *Bmp4* expression (and death) is regulated by the combination of WNT signalling and a PCD-inducing signal diffusing from the even-numbered rhombomeres.

Once *Bmp4* expression is initiated, it acts on the odd-numbered rhombomeres to induce *Msx2* and PCD (Graham et al., 1994). In contrast, when BMP4 protein is added to even-numbered rhombomeres, they do not undergo PCD (Graham et al., 1994). Consequently, BMP4 alone is unable to cause PCD in the presence of cSFRP2. Furthermore, *Msx2* gain-of-function studies have shown that *Msx2* is capable of inducing PCD within the even-numbered rhombomeres (Takahashi et al., 1998). This suggests that another, WNT-dependent factor is required to work in conjunction with BMP4 to initiate the *Msx2* and PCD.

We propose that the apoptotic program in the rhombencephalon is initiated by WNT signalling (Fig. 6). The ubiquitous expression of the WNT antagonist *cSfrp2* in the early hindbrain initially prevents PCD. Later in rhombencephalic development, *cSfrp2* expression becomes downregulated in the odd-numbered rhombomeres. In precise correlation with *cSfrp2* down-regulation, PCD becomes detectable in the odd-numbered rhombomeres (Lumsden et al., 1991). Presumably, the lack of cSFRP2 in the odd-numbered rhombomeres allows WNT to act in combination with the diffusible signal from the even-numbered rhombomeres to induce *Bmp4* expression. BMP4, in turn, acts with a WNT-dependent molecule (possibly TCF4 or JNK) to activate *Msx2* expression, and thus an autocrine loop induces PCD in the odd-numbered rhombomeres.

We are grateful to Frank Schubert for critical reading of this manuscript. We wish to thank Tony Brown for his generous gift of the retroviral *Wnt1* construct, Cliff Tabin for *Wnt3a* virus and for the *Tcf4* cDNA, David Wilkinson for the *Krox20* cDNA, Atsushi Kuroiwa for the *Hoxb*2 cDNA, Ivor Mason for the *Fgf*8 cDNA, and Anthony Graham for the *Msx2* cDNA. We also thank Jon Gilthorpe for his retroviral EGFP construct, and for his technical help with the electroporator, also Iano Campbell and Amata Hornbruch for their excellent technical help. This work was supported by the European Union, the Wellcome Trust, and the Medical Research Council.

REFERENCES

Augustine, K., Liu, E. T. and Sadler, T. W. (1993). Antisense attenuation of Wnt1 and Wnt3a expression in whole embryo culture reveals roles for these genes in craniofacial, spinal cord, and cardiac morphogenesis. *Dev. Genet.* **14**, 500-520.

Baker, J., Beddington, R. and Harland, R. (1999). Wnt signalling in *Xenpus* embryos inhibits *Bmp4* expression and activates neural development. *Genes Dev.* **13**, 3149-3159.

Basu, S. and Kolesnick, R. (1998). Stress signals for apoptosis: Ceramide and c-Jun kinase. *Oncogene* **17**, 3277-3285.

Birgbauer, E., Sechrist, J., Bronner-Fraser, M. and Fraser, S. (1995). Rhombomeric origin and rostracaudal reassortment of neural crest cells revealed by intravital microscopy. *Development* **121**, 935-945.

Boutros, M., Paricio, N., Strutt, D. I. and Mlodzik, M. (1998). Dishevelled activates JNK and discriminates between JNK pathways in planar polarity and wingless signalling. *Cell* **94**, 109-18.

Brannon, M., Gomperts, M., Sumoy, L., Moon, R. T. and Kimelman, D. (1997). A beta-catenin/XTCF3 complex binds to the siamois promoter to regulate dorsal axis specification in Xenopus. *Genes Dev.* **11**, 2359-2370.

Brunner, E., Peter, O., Schwelzer, L. and Basler, K. (1997). Pangolin encodes a Lef1 homologue that acts downstream of Armadillo to transduce the Wingless signal in Drosophila. *Nature* **385**, 829-833.

Buckland, R. A., Collinson, J. M., Graham, E., Davidson, D. R. and Hill, R. E. (1998). Antagonistic effects of FGF4 on BMP induction of apoptosis and chondrogenesis in the chick limb bud. *Mech. Dev.* **71,** 143-150.

Chang, J. T., Esumi, N., Moore, K., Li, Y., Zhang, S., Chew, C., Goodman, B., Rattner, A., Moody, S., Stetten, G., Campochiaro, P. A. and Zack, D. J. (1999). Cloning and characterization of a secreted frizzled-related protein that is expressed by the retinal pigment epithelium. *Hum. Mol. Genet.* **8**, 575-583.

Cho, E. and Dressler, G. (1998). TCF4 binds beta-catenin and is expressed in distinct regions of the embryonic brain and limbs. *Mech. Dev.* **77**, 9-18.

Couly, G., Grapin-Botton, A., Coltey, P. and La Douarin, N. M. (1996). The regeneration of the cephalic neural crest, a problem revisited: The regenerating cells originate from the contralateral or from the anterior and posterior neural fold. *Development* **122,** 3393-3407.

Dorsky, R. I., Moon, R. T. and Raible, D. W. (1998). Control of NC cell fate by the Wnt signalling pathway. *Nature* **396**, 370-372.

Eastman, Q. and Grosschedl, R. (1999). Regulation of LEF1/TCF transcription factors by Wnt and other signals. *Curr. Opin. Cell Biol.* **11**, 233-240.

Farlie, P., Kerr, R., Thomas, P., Symes, T., Minichiello, J., Hearn, C. and Newgreen, D. (1999). A paraxial exclusion zone creates patterned cranial neural crest cell outgrowth adjacent to rhombomeres 3 and 5. *Dev. Biol.* **213,** 70-84.

Ferrari, D., Lichtler, A., Pan, Z., Dealy, C., Upholt, W. and Kosher, R. (1998). Ectopic expression of Msx-2 in posterior limb bud mesoderm impairs limb morphogenesis while inducing BMP-4 expression, inhibiting cell proliferation, and promoting apoptosis. *Dev. Biol.* **197,** 12-24.

Finch, P. W., He, X., Kelley, M. J., Uren, A., Schaudies, R. P., Popescu, N. C., Rudikoff, S., Aaronson, S. A., Varmus, H. E. and Rubin, J. S. (1997). Purification and molecular cloning of a secreted, Frizzled-related antagonist of Wnt action. *Proc. Natl. Acad. Sci. USA* **94**, 6770-6775.

Foerst-Potts, L. and Sadler, T. (1997). Disruption of Msx-1 and Msx-2 reveals roles for these genes in craniofacial, eye, and axial development. *Dev. Dyn.* **209,** 70-84.

Francis, P., Richardson, M., Brickell, P. and Tickle, C. (1994). Bone morphogenetic proteins and a signalling pathway that controls patterning in the developing chick limb. *Development* **120**, 209-218.

Fraser, S., Keynes, R. and Lumsden, A. (1990). Segmentation in the chick embryo hindbrain is defined by cell lineage restrictions. *Nature* **334,** 431-435.

Ganan, Y., Macias, D., Basco, R. D., Merino, R. and Hurle, J. M. (1998). Morphological diversity of the avian foot is related with the pattern of msx gene expression in the developing autopod. *Dev. Biol.* **196,** 33-41.

Ganan, Y., Macias, D., Duterque-Coquillaud, M., Ros, M. and Hurle, J. (1996). Role of TGFβs and BMPs as signals controlling the position of the digits and the areas of interdigital cell death in the developing chick limb autopod. *Development* **122,** 2349-2357.

Graham, A., Francis-West, P., Brickell, P. and Lumsden, A. (1994). The signalling molecule BMP4 mediates apoptosis in the rhombencephalic NC. *Nature* **372**, 684-686.

Graham, A. Heyman, I. and Lumsden, A. (1993). Even-numbered rhombomeres control the apoptotic elimination of neural crest cells from odd-numbered rhombomeres in the chick hindbrain. *Development* **119**, 233-245.

Graham, A., Koentges, G. and Lumsden, A. (1996). NC apoptosis and the establishment of craniofacial pattern: an honorable death. *Mol. Cell. Neurosci.* **8**, 76-83.

Grasl-Kraupp, B., Ruttkay-Nedecky, B., Koudelka, H., Bukowska, K., Bursch, W. and Schulte-Hermann, R. (1995). In situ detection of fragmented DNA (TUNEL) fails to discriminate among apoptosis, necrosis, and autolytic death: a cautionary note. *J. Hepatology* **21**, 1465-1468.

Grove, E., Tole, S., Limon, J., Yip, L. and Ragsdale, C. W. (1998). The Hem of the embryonic cerebral cortex is defined by the expression of multiple Wnt genes and is compromised in the Gli3-deficient mice. *Development* **125**, 2315-2325.

Hamburger, V. and Hamilton, H. (1951). A series of normal stages in the development of the chick embryo. *J. Morphol.* **88**, 49-92.

Hays, R., Gibori, G. B. and Bejsovec, A. (1997). Wingless signaling generates pattern through two distinct mechanisms. *Development* **124**, 3727-3736.

Hoang, B. H., Thomas, J. T., Abdul-Karim, F. W., Correia, K. M., Conlon, R. A., Luyten, F. P. and Ballock, R. T. (1998). Expression pattern of two Frizzled-related genes, Frzb-1 and Sfrp-1, during mouse embryogenesis suggests a role for modulating action of Wnt family members. *Dev. Dynam.* **212**, 364-372.

Hollyday, M., McMahon, J. and McMahon, A. (1995). Wnt expression patterns in chick embryo nervous system. *Mech. Dev.* **52**, 9-25.

Hume, C. and Dodd, J. (1993). Cwnt-8C: a novel Wnt gene with a potential role in primative streak formation and hindbrain organization. *Mech. Dev.* **119**, 1147-1160.

Ikeya, M., Lee, S. M. K., Johnson, J. E., McMahon, A. P. and Takada, S. (1997). Wnt signalling required for expansion of neural crest and CNS progenitors. *Nature* **389,** 968-970.

Jacobson, M., Weil, M. and Raff, M. C. (1997). Programmed cell death in animal development. *Cell* **88**, 347-354.

Jeffs, P., Jaques, K. and Osmond, M. (1992). Cell death in cranial neural crest development. *Anat. Embryol.* **185,** 583-588.

Katagiri, T., Boorla, S., Frendo, J., Hogan, B. and Karsenty, G. (1998). Skeletal abnormalities in doubly heterozygous Bmp4 and Bmp7 mice. *Dev. Genet.* **22,** 340-348.

Kengaku, M., Capdevila, J., Rodriguez-Esteban, C., De La Pena, J., Johnson, R. L., Belmonte, J. C. I. and Tabin, C. J. (1998). Distinct WNT pathways regulating AER formation and dorsoventral polarity in the chick limb bud. *Science* **280**, 1274-77.

Köntges, G. and Lumsden, A. (1996). Rhombencephalic NC segmentation is preserved throughout craniofacial ontogeny. *Development* **122**, 3229-3242.

Korinek, V., Barker, N., Willert, K., Molenaar, M., Roose, J., Wagenaar, G., Markman, M., Lamers, W., Destree, O. and Clevers, H. (1998). Two members of the TCF family implicated in Wnt/beta-catenin signalling during embryogenesis in the mouse. *Mol. Cell. Biol.* **18**, 1248-1256.

Kuan, C., Yang, D., Roy, D., Davis, R., Rakic, P. and Flavell, R. (1999). The Jnk1 and Jnk2 protein kinases are required for regional specific apoptosis during early brain development. *Cell* **22**, 667-676.

Kulesa, P. M. and Fraser, S. E. (1998). Neural crest cell dynamics revealed by time-lapse video microscopy of whole embryo chick explant cultures. *Dev. Biol.* **204,** 327-344.

Kulesa, P. M. and Fraser, S. E. (2000). In ovo time-lapse analysis of chick hindbrain neural crest cell migration shows cell interactions during migration to the branchial arches. *Development* **127,** 1161-1172.

LaBonne, C. and Bronner-Fraser, M. (1998). Neural crest induction in Xenopus: evidence for a two-signal model. *Development* **125,** 2403-2414.

Ladher, R. K., Church, V. L., Allen, S., Robson, L., Abdelfattah, A., Brown, N. A., Hattersley, G., Rosen, V., Luyten, F. P., Dale, L., Francis-West, P. H. (2000). Cloning and expression of the Wnt antagonists Sfrp2 and FrzB during chick development. *Dev. Biol.* **218**, 183-198.

Lee, C. S., Buttitta, L. A., May, N. R., Kispert, A. and Fan, C. M. (2000). SHH-N upregulates Sfrp2 to mediate its competitive interaction with WNT1 and WNT4 in the somitic mesoderm. *Development* **127**, 109-118.

Leimeister, C., Bach, A. and Gessler, M. (1998). Developmental expression patterns of mouse sFRP genes encoding members of the secreted frizzled related protein family. *Mech. Dev.* **75**, 29-42.

Lescher, B., Haenig, B. and Kispert, A. (1998). SFRP-2 is a target of the Wnt-4 signaling pathway in the developing metanephric kidney. *Dev. Dynam.* **213**, 440-451.

Leynes, L., Bouwmeester, T., Kim, S. H., Piccolo, S. and De Robertis, E. M. (1997). Frzb-1 is a secreted antagonist of Wnt signalling expressed in the spemann organiser. *Cell* **88**, 747-756.

Li, L., Yuan, H., Xie, W., Mao, J., Caruso, A. M., McMahon, A., Sussman, D. J. and Wu, D. (1999). Dishevelled proteins lead to two signaling pathways: Regulation of LEF- 1 and c-Jun N-terminal kinase in mammalian cells. *J. Biol. Chem.* **274**, 129-134.

Lumsden, A. (1990). The cellular basis of segmentation in the developing hindbrain. *Trends Neurosci.* **13**, 329-334.

Lumsden, A. (1991). Cell lineage restrictions in the chick embryo hindbrain. *Phil. Trans. R.Soc. Lon. B* **331,** 281-286.

Lumsden, A., Sprawson, N. and Graham, A. (1991). Segmental origin and migration of NC cells in the hindbrain region of the chick embryo. *Development* **113**, 1281-91.

Maden, M., Graham, A., Gale, E., Rollinson, C. and Zile, M. (1997). Positional apoptosis during vertebrate CNS development in the absence of endogenous retinoids. *Development* **124,** 2799-2805.

Mahmood, R., Bresnick, J., Hornbruch, A., Mahony, C., Morton, N., Colquhoun, K., Martin, P., Lumsden, A., Dickson, C. and Mason, I. (1995). A role for FGF-8 in the initiation and maintenance of vertebrate limb bud outgrowth. *Curr. Biol.* **5**, 797-806.

Marazzi, G., Wang, Y. and Sassoon, D. (1997). Msx2 is a transcriptional regulator in the BMP4-mediated programmed cell death pathway. *Dev. Biol.* **186**, 127-138.

McMahon, A. P. and Bradley, A. (1990). The Wnt1 (int-1) proto-oncogene is required for development of a large region of the mouse brain. *Cell* **62**, 1073-1085.

Melkonyan, H., Chang, W., Shapiro, J. P., Mahadevappa, M., Fitzpatrick, P., Kiefer, M., Tomei, L. D. and Umansky, S. (1997). SARPs: a family of secreted apoptosis related proteins. *Proc. Natl. Acad. Sci. USA* **94**, 13636-13641.

Merino, R., Ganan, Y., Macias, D., Rodriguez-Leon, J. and Hurle, J. M. (1999). Bone morphogenetic proteins regulate interdigital cell death in the avian embryo. *Annals NY Acad. Sci.* **887**, 120-132.

Moon, R. T., Brown, J. D. and Torres, M. (1997). WNTs modulate cell fate and behavior during vertebrate development. *Trends Genet.* **13**, 157-162.

Morgan, B. and Fekete, D. (1996). Manipulating gene expression with replication-competent retroviruses. In *Methods in Avian Embryology*, (ed. M. Bronner-Fraser) London: Academic Press.

Nieto, M. A., Sechrist, J., Wilkinson, D. G. and Bronner-Fraser, M. (1995). Relationship between spatially restricted Krox-20 gene expression in branchial neural crest and segmentation in the chick embryo hindbrain. *EMBO J.* **14,** 1697-1710.

Parr, B. A. and McMahon, A. P. (1994). Wnt genes and vertebrate development. *Curr. Opin. Genet. Dev.* **4**, 523-528.

Rattner, A., Hsieh, J. C., Smallwood, P. M., Gilbert, D. J., Copeland, N. G., Jenkins, N. A. and Nathans, J. (1997). A family of secreted proteins contains homology to the cysteine-rich ligand-binding domain of frizzled receptors. *Proc. Natl. Acad. Sci. USA* **94**, 2859-2863.

Rudnicki, J. A. and Brown, A. M. C. (1997). Inhibition of chondrogenesis by *Wnt1* gene expression in vivo and in vitro. *Dev. Biol.* **185**, 104-118.

Saint-Jeannet, J. P., He, X., Varmus, H. E. and Dawid, I. B. (1997). Regulation of dorsal fate in the neuraxis by Wnt1 and Wnt3a. *Proc. Natl. Acad. Sci. USA* **94**, 13713-13718.

Salic, A. N., Kroll, K. L., Evans, L. M. and Kirschner, M. W. (1997). Sizzled: A secreted Xwnt8 antagonist expressed in the ventral marginal zone of *Xenopus* embryos. *Development* **124**, 4739-4748.

Sechrist, J., Serbedzija, G. N., Scherson, T., Fraser, S. E., Bronner-Fraser, M.(1993). Segmental migration of the hindbrain neural crest does not arise from its segmental generation. *Development* **118**, 691-703.

Serbedzija, G., Dickinson, M. and McMahon, AP. (1996). Cell death in the CNS of the Wnt1 mutant mouse. *J. Neurobiol.* **31**, 275-82.

Shirozu, M., Tada, H., Tashiro, K., Nakamura, T., Lopez, N., Nazarea, M., Hamada, T., Sato, T., Nakano, T. and Honjo., T. (1996). Characterisation of novel secreted and membrane proteins isolated by the signal sequence trap method. *Genomics* **37**, 273-280.

Shulman, J. M., Perrimon, N. and Axelrod, J. D. (1998). Frizzled signaling and the developmental control of cell polarity. *Trends Genet.* **14**, 452-458.

Takahashi, K., Nuckolls, G., Tanaka, O., Semba, I., Takahashi, I., Dashner, R., Shum, L. and Slavkin, H. (1998). Adenovirus-mediated ectopic expression of Msx2 in even-numbered rhombomeres induces apoptotic elimination of cranial neural crest cells in ovo. *Development* **125,** 1627-1635.

Tewari, M., Quan, L. T., K, O. R., Desnoyers, S., Zeng, Z., Beidler, D. R., Poirier, G. G., Salvesen, G. S. and Dixit, V. M. (1995). Yama/CPP32 beta, a mammalian homolog of CED-3, is a CrmA-inhibitable protease that cleaves the death substrate poly(ADP-ribose) polymerase. *Cell* **81,** 801-809.

Wang, S., Krinks, M., Lin, K., Luyten, F. P. and Moos, M., Jr. (1997). Frzb, a secreted protein expressed in the Spemann organizer, binds and inhibits Wnt-8. *Cell* **88**, 757-766.

Wang, S., Krinks, M. and Moos, M. J. (1997). Frzb-1, an antagonist of Wnt1 and Wnt-8, does not block signaling by Wnts −3A, −5A, or −11. *Biochem. Biophys. Res. Commun.* **236**, 502-504.

Weil, M., Jacobson, M. and Raff, M. (1997). Is programmed cell death required for neural tube closure. *Curr. Biol.* **7**, 281-284.

Wilder, E. L. and Perrimon, N. (1995). Dual functions of wingless in the *Drosophila* leg imaginal disc. *Development* **121**, 477-488.

Wilkinson, D. (1992). *In-situ Hybridisation* Oxford: IRL Press.

Winograd, J., Reilly, M. P., Roe, R., Lutz, J., Laughner, E., Xu, X., Hu, L., Asakura, T., Vander Kolk, C., Strandberg, J. D. and Semenza, G. L. (1997). Perinatal lethality and multiple craniofacial malformations in MSX2 transgenic mice. *Hum. Mol. Gen*et. **6,** 369-379.

Wodarz, A. and Nusse, R. (1998). Mechanisms of Wnt signaling in development. *Annu. Rev. Cell Dev. Biol.* **14**. 58-88.

Wolf, V., Ke, G., Dharmarajan, A. M., Bielke, W., Artuso, L., Saurer, S. and Friis, R. (1997). DDC-4, an apoptosis associated gene, is a secreted frizzled relative. *FEBS Letts* **417**, 385-389.

Xu, Q., P. A., Amore, P. A. D. and Sokol, S. Y. (1998). Functional and biochemical interactions of Wnts with FrzA, a secreted Wnt antagonist. *Development* **125**, 4767-4776.

Yokouchi, Y., Sakiyama, J., Kameda, T., Iba, H., Suzuki, A., Ueno, N. and Kuroiwa, A. (1996). BMP-2/-4 mediate programmed cell death in chicken limb buds. *Development* **122,** 3725-3734.

Yoshida, H., Kong, Y., Yoshida, R., Elia, AJ., Hakem, A., Hakem, R., Penninger, JM. and Mak, TW. (1998). Apaf1 is required for mitochondrial pathways of apoptosis and brain development. *Cell* **94**, 739-750.

Yoshikawa, Y., Fujimori, T., McMahon, A. P. and Takada, S. (1997). Evidence that absence of Wnt3a signaling promotes neuralization instead of paraxial mesoderm development in the mouse. *Dev. Biol*. **183**, 234-242.

Yuan, J. and Horvitz, H. (1990). The Caenorhabditis elegans genes ced-3 and ced-4 act cell autonomously to cause programmed cell death. *Dev. Biol.* **138,** 33-41.

Zou, H. and Niswander, L. (1996). Requirement for BMP signalling in interdigital apoptosis and scale formation. *Science* **272,** 738-741.

Zhou, Z., Wang, J., Han, X., Zhou, J. and Linder, S. (1998). Up-regulation of human secreted frizzled homolog in apoptosis and its down-regulation in breast tumours. *Int. J. Cancer* **78**, 95-99.